Available online at www.sciencedirect.com
SCIENCE DIRECT®
Surface & Coatings Technology xx (2005) xxx – xxx
SURFACE & COATINGS TECHNOLOGY
www.elsevier.com/locate/surfcoat

Comparative properties of titanium oxide biomaterials grown by pulsed vacuum arc plasma deposition and by unbalanced magnetron sputtering

Y.X. Leng *, J.Y. Chen, J. Wang, G.J. Wan, H. Sun, P. Yang, N. Huang

School of Materials Science and Engineering, Southwest Jiaotong University, Chengdu, 610031, China

Received 24 September 2005; accepted in revised form 7 November 2005

Abstract

The aim of the paper is to characterize titanium oxide films synthesized by unbalanced magnetron sputtering and metal vacuum arc deposition, as well as to test the microstructure, composition, sheet resistance and blood compatibility. With increasing oxygen inlet, the rutile TiO_2 can be synthesized in both processes. The sheet resistance of the samples increases with higher oxygen pressure and it shows a sharp increase when only rutile TiO_2 exists in the films, a similar tendency was found for pulsed vacuum arc plasma deposition and unbalanced magnetron sputtering methods. The films synthesized by the unbalanced magnetron sputtering and pulsed vacuum arc deposition sample contain the rutile phase and have a similar composition, but the microstructures like grain size and roughness are different. These will affect the semiconductivity and the surface energy, and these properties affected their blood compatibility and made their blood compatibility more different. The platelet adhesion behavior of rutile TiO_2 synthesized by unbalanced magnetron sputtering is better than the one synthesized by pulsed vacuum arc deposition.
© 2005 Elsevier B.V. All rights reserved.

Keywords: Titanium oxide; Blood compatibility; Pulsed vacuum arc plasma deposition; Unbalanced magnetron sputtering; Microstructure

1. Introduction

Ti and its alloys are thought to be highly biocompatible materials, and their clinical applications are becoming increasingly frequent. The excellent biocompatibility of titanium and its alloys is associated with the properties of their surface oxide [1]. However, there are some reports demonstrating that the natural oxide film may not be sufficiently protective in the aggressive biologic environment, and there have recently been some clinical papers reporting hypersensitivity and allergic reactions to Ti [2,3]. One way to solve this problem is depositing ceramic thin films [4]. Inert ceramic surfaces exhibit minimal ion release [5]. Rutile type titanium oxide ceramics and thermally oxidized TiO_2 and TiO_{2-x} prepared by ion beam assisted deposition generally have good blood compatibility, and it has been found that when the oxide thickness exceeds 40 nm, its blood compatibility is better than that of low-temperature isotropic pyrolytic carbon (LTIC) [6–10]. In this work, titanium oxide films were deposited on Si (100) by pulsed vacuum arc plasma deposition [11,12] and unbalanced magnetron sputtering [13] methods at different O_2 pressure, and their structure, chemical composition, sheet resistance and blood compatibility were investigated.

2. Experiment

For unbalanced magnetron sputtering deposition (UBM), the chamber was evacuated to a typical background pressure of 10^{-4} Pa by a turbomolecular pumping unit. TiO_x thin films were prepared on Si (100) substrate by reactive DC magnetron sputtering from a metallic titanium target (purity 99.9%) in a mixed Ar/O_2 atmosphere. The target-to-substrate distance was 10 cm. The discharge current was kept constant at 3 A which corresponds to a power density of 5 W cm^{-2}. Working gases were Ar and O_2 whose flow rates were separately controlled by mass flow controllers. The depositions were performed at a total pressure of 0.5 Pa. During the deposition the substrates were heated to ~520–570 K. The ratio between the oxygen and argon ($O_2/(Ar+O_2)$) varied between 6.6% and 28%. Prior to the sputter deposition step of the films, a movable shutter

* Corresponding author. Tel.: +86 28 87600728/66371772; fax: +86 28 87600625.
E-mail address: yxleng@263.net (Y.X. Leng).

0257-8972/$ - see front matter © 2005 Elsevier B.V. All rights reserved.
doi:10.1016/j.surfcoat.2005.11.074

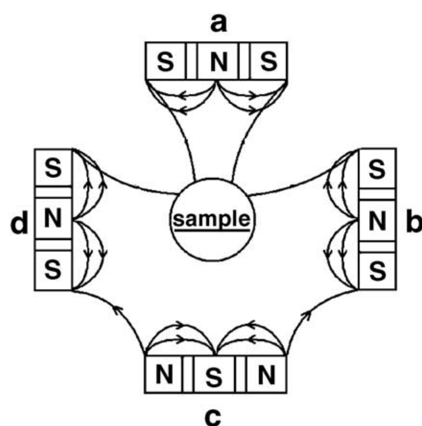

Fig. 1. Schematic drawing of a four-cathode unbalanced magnetron sputtering system showing the magnetic fields between cathodes (in this experiment, only cathode C was triggered and distance between target C and sample was 10 cm).

was interposed between the target and the substrates and the target was presputtered in pure argon atmosphere for 5 min in order to remove the surface oxide layer on the titanium target. The substrate bias voltage was −50 V. The deposition time was 15 min. The thickness of the samples has been measured with a profilometer (Alpha step 500). The film thickness was in the range of ~200–1000 nm depending on $O_2/(Ar+O_2)$ ratio. In order to increase the ion flux density and ion/atom ratio, we change the arrangement of the magnetic field, as shown in Fig. 1. The ion flux density in our experiment was about 2.3 mA/cm^2.

For pulsed vacuum arc plasma deposition, titanium oxide films were deposited on silicon (100) substrates using metal vacuum arc deposition. The metal vacuum arc deposition system has been described previously [11,12]. A Ti cathode (purity: 99.99%) 14 mm in diameter was mounted onto the metal vacuum arc plasma source. The titanium plasma was generated in the metal arc source and diffused into the vacuum chamber via a magnetic duct to eliminate deleterious macro-particles. The titanium oxide films were deposited as a function of oxygen gas pressure. The base pressure of the system was 2×10^{-3} Pa. The deposition conditions were: metal arc pulse frequency=60 Hz, metal arc pulse duty=1 ms, metal arc current=180 A, metal arc main current=0.8 A, substrate voltage=−60 V, deposition rate: ~100 Å/min, oxygen flow rate=3, 10, 15, 30 sccm, which code with A1, A2, A3, A4. The film thickness was about 6000–7000 Å tested by a step profilometer. During the deposition the substrates were heated to 673 K. The experimental arrangement and deposition technique are listed in Table 1.

The film composition was determined by X-ray photoelectron spectroscopy (XPS), and surface morphology was studied by atomic force microscopy (AFM). The phase and crystal structure of films were identified by X-ray diffraction (XRD) with a Philip X'Pert (CuKα radiation). The microstructure was also studied by a Renishaw RM 3000 Micro-Raman system at room temperature using a 25 mW He–Ne laser (633 nm). The sheet resistance of the titanium oxide films was determined using four-point probe measurements. Platelet adhesion tests were performed on #S5, #A3 and low-temperature isotropic pyrolytic carbon (LTIC). Blood was obtained from a healthy adult volunteer. The whole blood was collected in an acid citrate dextrose (ACD) medium. After centrifugation, red cells and platelets were speared and a platelet-rich plasma was obtained. The samples were immersed into the platelet-rich plasma and incubated at 37 °C for 10 min and 1 h, respectively. After rinsing, fixing and critical point drying, the specimens were examined using scanning electron microscopy (SEM) and optical microscopy. The quantity and morphology of the adhered platelet were examined to study the surface thrombogenicity. Twenty different locations were chosen at random to obtain a good statistical average.

3. Results and discussion

XRD patterns in a grazing angle ($\theta=3°$) configuration of the films deposited at different $O_2/(Ar+O_2)$ ratio by UBM sputtering are shown in Fig. 2. When $O_2/(Ar+O_2)$ ratio is lower than 11.7%, the Ti_2O, TiO and Ti_2O_3 can be observed. It reveals that the onset of each different phase takes place at specific $O_2/(Ar+O_2)$ ratio. Our investigations showed that the films deposited by UBM sputtering have a polycrystalline and generally rutile structure as $O_2/(Ar+O_2)$ reaching 11.7%, as shown in Fig. 2.

Raman spectra of the UBM sputtering films are presented in Fig. 3. No bands are detected in the spectrum of the film obtained at 6.6% $O_2/(Ar+O_2)$ ratio. XRD results showed that Ti_2O and TiO coexisted at 6.6% $O_2/(Ar+O_2)$ ratio. Because Ti_2O and TiO compounds are not Raman active [14], they are not detectable with Raman technique. At 9.3% $O_2/(Ar+O_2)$ ratio, the existence of Ti_2O_3 is confirmed by the presence of bands between 200 and 350 cm^{-1}, these bands seem to belong to crystalline Ti_2O_3. This can be confirmed by XRD results: the Ti_2O_3 and TiO coexisted at 9.3% $O_2/(Ar+O_2)$ ratio. Afterwards, at the samples deposited from 11.7% to 28% $O_2/(Ar+O_2)$ ratio, the Raman spectra of the films show the same three lines at 230, 434 and 606 cm^{-1} which are characteristic of the rutile phase, consistent with XRD results. It also showed that the Raman

Table 1
Processing conditions of unbalanced magnetron sputtering (S) and pulsed vacuum arc plasma deposition (A) samples

Sample no.	S1	S2	S3	S4	S5	S6	S7	S8	A1	A2	A3	A4
O_2 inlet (sccm)	5	7.2	10.1	10.6	12	14.4	20	30	3	10	15	30
Ar inlet (sccm)	71	70.4	76.2	73.6	75	75.8	79.4	76	Pulsed vacuum arc plasma deposition			
$O_2/(Ar+O_2)$	6.6%	9.3%	11.7%	12.6%	13.8	16%	17%	28%				
Thickness (nm)	960	970	740	555	490	407	210	195				
Unbalanced magnetron sputtering deposition												

ARTICLE IN PRESS

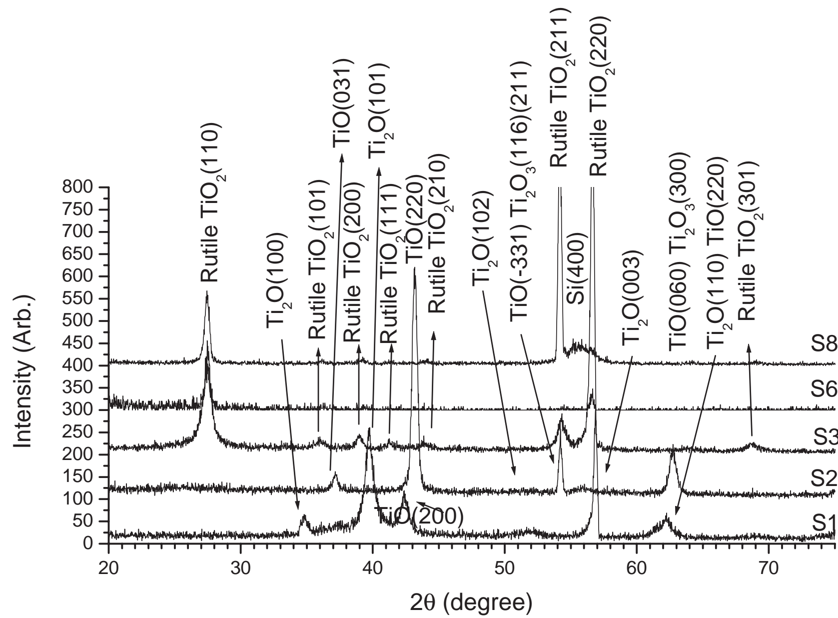

Fig. 2. X-ray diffraction patterns of the titanium oxide films deposited at different $O_2/(Ar+O_2)$ ratio by unbalanced magnetron sputtering in a grazing angle ($\theta=3°$) configuration.

peaks intensity of the rutile phase decreased and the peaks intensity of Si located at 302 and 517 cm^{-1} [15] increased as the $O_2/(Ar+O_2)$ ratio increased. This resulted in decreasing film thickness. As the $O_2/(Ar+O_2)$ ratio increased, the films deposition rate decreased.

Fig. 4 shows the XRD pattern of the films deposited by pulsed vacuum arc plasma deposition. As the oxygen inlet is less than 10 sccm, the suboxide Ti_4O_7 phase exists. And if the oxygen inlet is more than 10 sccm, only rutile TiO_2 is detected. This tendency was similar to that for the film deposited by UBM sputtering with the ratio of $O_2/(Ar+O_2)$ reaching 11.7%. But the half-height peak width of the pulsed vacuum arc plasma deposited rutile (110) direction is slightly bigger than the UBM sputtering deposited rutile (110). This means that the pulsed vacuum arc plasma deposition rutile have smaller grains than the sputtering one. This can be confirmed by AFM. Fig. 5 showed the AFM images of the pulsed vacuum arc plasma deposition rutile films (#A2) and unbalanced magnetron sputtering deposition sample (#S3). As shown in Fig. 5(a), particles of about 130–160 nm arrayed uniformly on the film surface. For unbalanced magnetron sputtering deposition sample (#S3), particles ranging from 170 to 230 nm can be

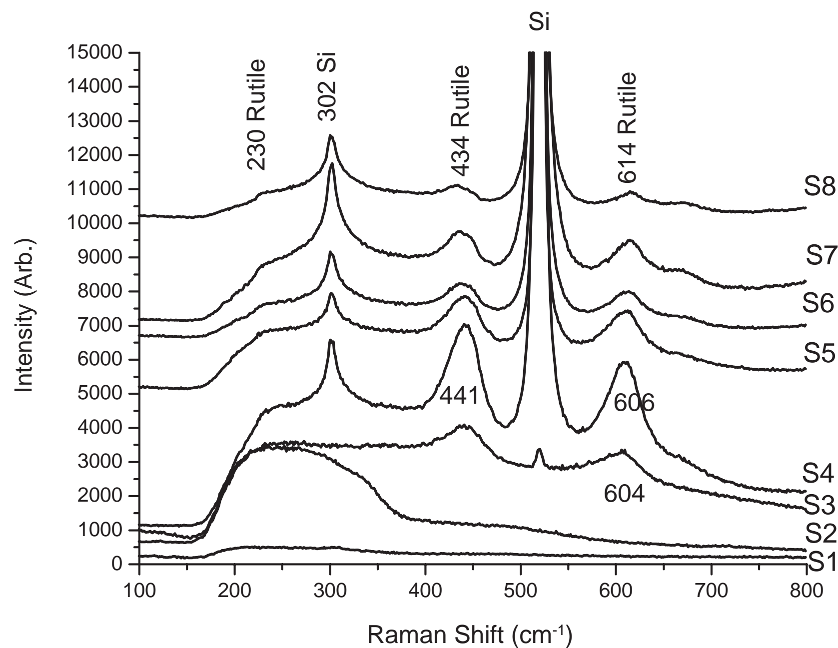

Fig. 3. Raman spectra of the unbalanced magnetron sputtering titanium oxide films synthesized at different $O_2/(O_2+Ar)$ ratio.

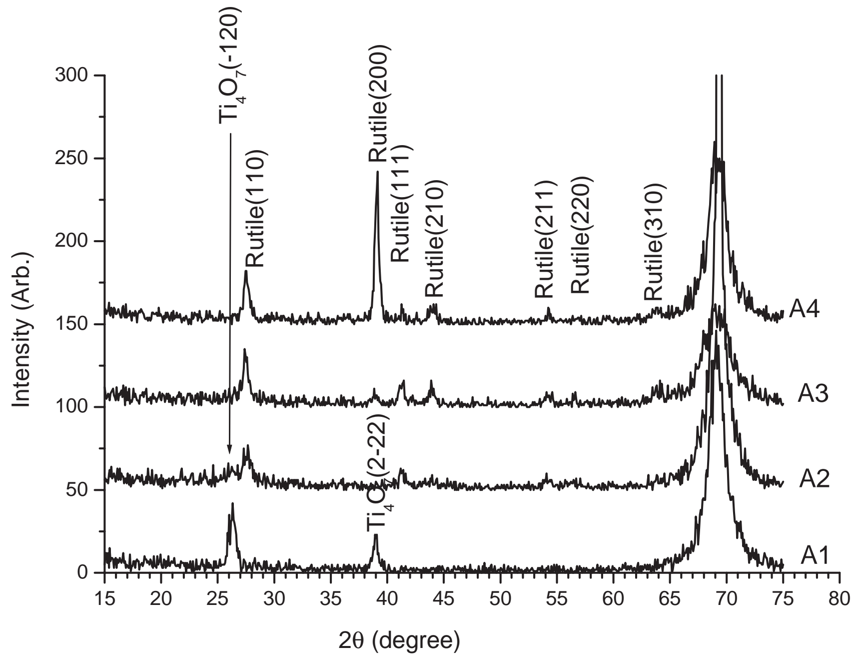

Fig. 4. The X-ray diffraction pattern of the titanium oxide films deposited by pulsed vacuum arc plasma deposition.

observed and the #S3 surface roughness (39.3 Å) is larger than pulsed vacuum arc plasma deposition one (12.6 Å). It is demonstrated that the films grown by pulsed vacuum arc plasma deposition are smoother. As we know, the energy of particles impinging into the substrate is an important parameter affecting the film surface morphology. For pulsed vacuum arc plasma

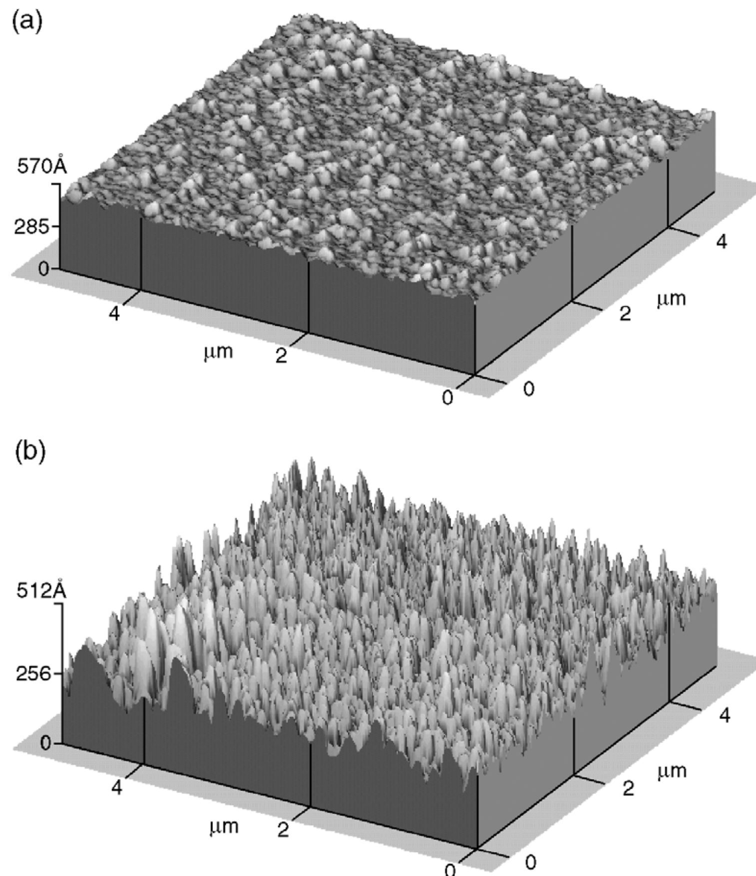

Fig. 5. The AFM images of the pulsed vacuum arc plasma deposition rutile films #A2 (a) and unbalanced magnetron sputtering deposition sample #S3 (b).

ARTICLE IN PRESS

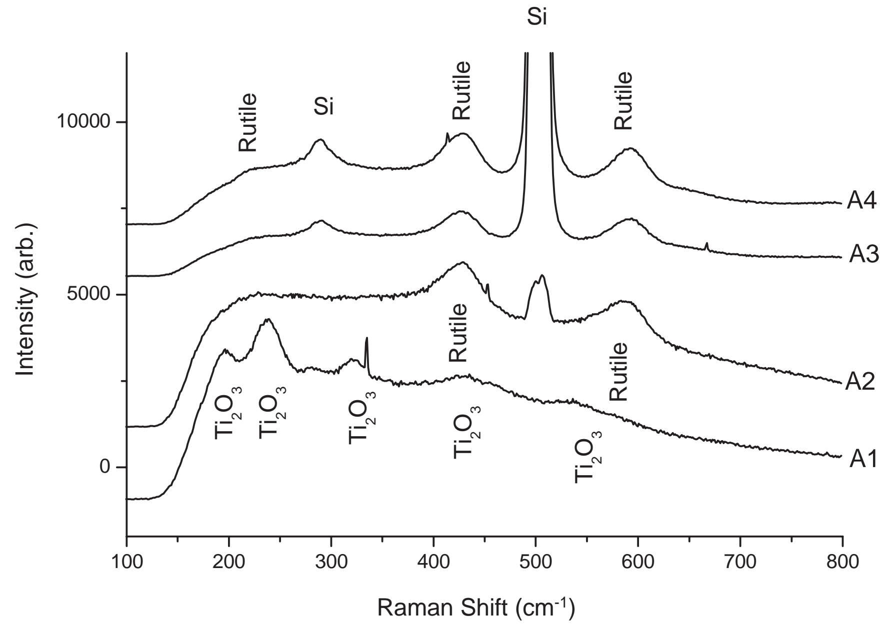

Fig. 6. Raman spectra of the pulsed vacuum arc plasma deposition titanium oxide films.

deposition, Ti ions have an initial kinetic energy of approximately 50 eV when they are generated in the metal vacuum arc plasma source. After they diffuse into the vacuum chamber via the magnetic duct, they are further accelerated by a −50 V bias, and thus the total energy is over 100 eV, depending on the charge state of the ions. Ti ions bombard the film and make the surface smooth. For UBM sputtering, though the argon and oxygen ion impinge on the films at a −50 V bias voltage, their mass is smaller than that of Ti, hence the bombardment energy and the bombardment effect are smaller than that of Ti ion. So the pulsed vacuum arc plasma deposition titanium oxides have a smoother surface.

Raman spectra of the pulsed vacuum arc plasma deposition titanium oxide films are presented in Fig. 6. At 3 sccm oxygen inlet, the existence of Ti_2O_3 is confirmed by the presence of bands 200, 238, 320 and 540, these bands seem to belong to crystalline Ti_2O_3 [14] and rutile TiO_2. This can be confirmed by XRD results: the suboxide Ti_4O_7 existed at 3 sccm oxygen inlet. Afterwards, the oxygen inlet increased from 10 to 30 sccm, the Raman spectra of the films show the same three lines at 223,

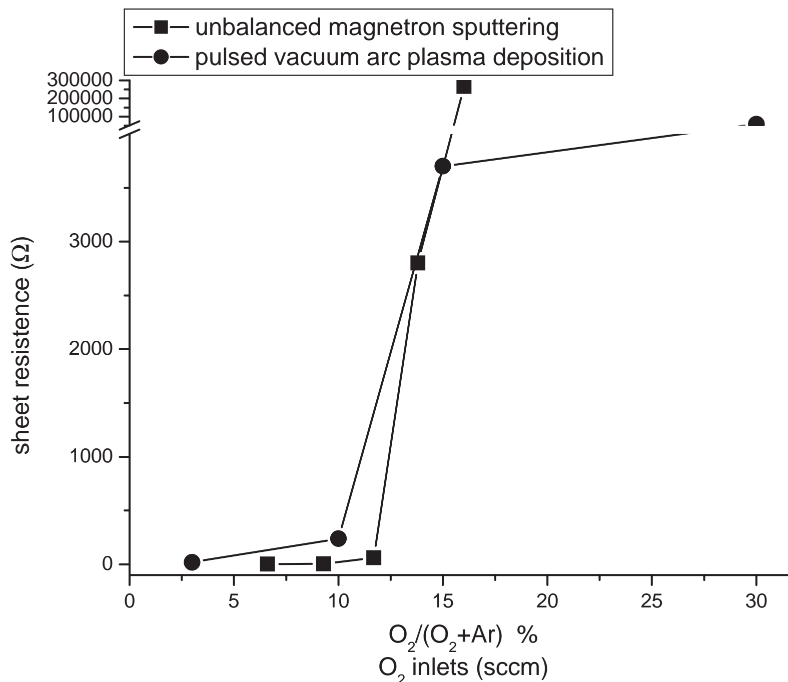

Fig. 7. The sheet resistance of the samples synthesized by pulsed vacuum arc plasma deposition and unbalanced magnetron sputtering.

ARTICLE IN PRESS

428 and 592 cm^{-1} which are characteristic of the rutile phase, consistent with XRD results.

The sheet resistance of the samples was measured and the results are shown in Fig. 7. In general, the sheet resistance of as-deposited samples increases with higher oxygen pressure. For UBM sputtering titanium oxide films, the sheet resistance of the samples shows a sharp increase when the $O_2/(O_2+Ar)$ ratio exceed 11.7% as shown in Fig. 7. When the $O_2/(O_2+Ar)$ ratio is less than 11.7%, there are TiO and Ti_2O_3 which are showed in Figs. 2 and 3, titanium suboxides and vacancies exist in the films and enhance electrical conduction. When the $O_2/(O_2+Ar)$ ratio is larger than 11.7%, only rutile TiO_2 phase exists and no suboxides can be found. Thus, the resistance increases sharply. For pulsed vacuum arc plasma deposition titanium oxide films, there are similar results; the sheet resistance of the samples shows a sharp increase when the O_2 inlet exceeds 10 sccm as shown in Fig. 7. When the O_2 inlet is less than 10 sccm, there is suboxide (Ti_4O_7) which is shown in Figs. 4 and 6. Bulk oxygen vacancies are known to generate shallow electron donors that contribute to the electrical conductivity of TiO_2 [16], so when the suboxide existed in the films, it made the film resistance smaller. When the O_2 inlet is larger than 10 sccm, only rutile TiO_2 phase exists and no suboxides can be found. Thus, the resistance increases sharply.

Adhered platelets are usually measured to assess hemocompatibility, and activation of platelets is a more important parameter indicating the interaction of blood with materials than the adhesion behavior [17–20]. In our experiments, the hemocompatibility of the stoichiometric titanium oxide (A3 and S5) was studied. XPS and XRD results show that the samples #A3 and #S5 were fully oxidized and only rutile existed in the films. Our platelet adhesion study illustrates that the number of adhered platelets is highest on #A3 and smallest on #S5 and LTIC, as shown in Fig. 8. It can be observed that the number of platelets adhered onto the #S5 film was markedly less than that on #A3. The degree of deformation (pseudopodium) and aggregation of the adhered platelets are also less on #S5. The blood compatibility of #S5 is better than that of #A3. The degree of deformation (pseudopodium) and aggregation of the adhered platelets on the #S5 samples are similar with those of LTIC for the incubation time of 120 min. Our data demonstrate that the blood compatibility of the #S5 samples is as good as that of LTIC, and is better than that of the #A3. #S5 and #A3 have a similar rutile TiO_2 microstructure and composition which have been investigated by XPS, Raman and XRD, why their blood compatibility is so different.

The interaction between blood and artificial materials is quite complicated and not well understood [17,18]. The material characteristics such as surface energy and semiconductivity play an important role in blood compatibility [17,18]. It is well known that in polycrystalline thin films transport mechanism of charge carriers is strongly influenced by crystallite size and the characteristics of grain boundaries [21–23]. Though the UBM sputtering sample #S5 and pulsed vacuum arc deposition sample #A3 contain the rutile phase and have a similar composition, they have different grain size and roughness, and this will affect the semiconductivity and the surface energy.

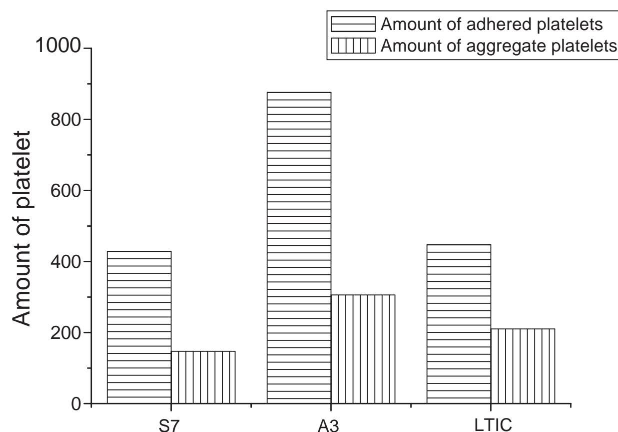

Fig. 8. Quantity of platelets adhered on titanium oxide film and LTIC (incubation time = 120 min).

And we supposed that UBM sputtering sample #S5 has certain electronic and structural states, this may inhibit adsorption of 'harmful' proteins such as fibrinogen or globulin onto the material surface and may be able to prevent the absorbed protein from denaturing. So the sample #5 has a better blood compatibility. We are investigating the relationship between the blood compatibility of titanium oxide and the electronic properties and will publish our results in the future.

4. Conclusions

Titanium oxides were deposited onto Si (100) substrates by pulsed vacuum arc plasma deposition and UBM sputtering methods. As oxygen inlet increases, the rutile TiO_2 can be synthesized, the sheet resistance of the samples increases with higher oxygen pressure and the sheet resistance of the samples shows a sharp increase when only rutile TiO_2 exists in the films. There are similar results for pulsed vacuum arc plasma deposition and UBM sputtering methods. Though the films synthesized by UBM sputtering and pulsed vacuum arc deposition samples contain the rutile phase and have a similar composition, they have different grain size and roughness; this will affect the semiconductivity and the surface energy and then their blood compatibility is more different. The platelet adhesion behavior of rutile TiO_2 synthesized by the UBM sputtering is better than the one synthesized by pulsed vacuum arc deposition. The relationship between the blood compatibility of titanium oxide and the electronic properties should be investigated further.

Acknowledgements

This work was jointly and financially supported by Natural Science Foundation of China (30400109) and Key Basic Research Program 2005CB623904.

References

[1] D. Velten, V. Biehl, F. Aubertin, B. Valeske, W. Possart, J. Breme, J. Biomed. Mater. Res. 59 (1) (2002) 18.

ARTICLE IN PRESS

[2] T. Sawase, A. Wennerberg, K. Baba, Y. Tsuboi, L. Sennerby, C.B. Johansson, T. Albrektsson, Clin. Implant Dent. Relat. Res. 3 (4) (2001) 221.
[3] M. Koike, H. Fujii, Biomaterials 22 (21) (2001) 2931.
[4] R. Hũbler, Surf. Coat. Technol. 116–119 (1999) 1111.
[5] W.R. Lacefield, Adv. Dent. Res. 13 (1999) 21.
[6] R. Ebert, M. Schaldach, Proc. World Congress on Med. Phys. Biomed. Eng., Hamburg, vol. 307, 1982.
[7] N. Huang, Y.R. Chen, J.M. Luo, J. Yi, R. Lu, J. Xiao, Z.N. Xue, X.H. Liu, J. Biomater. Appl. 8 (1994) 404.
[8] X.H. Liu, Z.H. Zheng, Z.Y. Zhou, N. Huang, P. Yang, G.J. Cai, Y.R. Chen, J. Biomater. Appl. 10 (4) (1996) 330.
[9] N. Huang, P. Yang, X. Chen, Y.X. Leng, X.L. Zeng, G.J. Jun, Z.H. Zheng, F. Zhang, Y.R. Chen, X.H. Liu, Biomaterials 19 (1998) 771.
[10] J. Li, Biomaterials 14 (1993) 229.
[11] Y.X. Leng, N. Huang, P. Yang, J.Y. Chen, H. Sun, J. Wang, G.J. Wan, X.B. Tian, R.K.Y. Fu, Surf. Coat. Technol. 156 (2002) 295.
[12] Y.X. Leng, N. Huang, P. Yang, J.Y. Chen, H. Sun, J. Wang, G.J. Wan, Y. Leng, P.K. Chu, Thin Solid Films 420–421 (2002) 408.
[13] William D. Sproul, Surf. Coat. Technol. 81 (1996) 1.
[14] A. Pérez del Pino, P. Serra, J.L. Morenza, Thin Solid Films 415 (2002) 201.
[15] A.V. Kolobov, K. Morita, K.M. Itoh, E.E. Haller, Appl. Phys. Lett. 81 (20) (2002) 3855.
[16] A.T. Paxton, L. Thien-Nga, Phys. Rev., B 57 (1998) 1579.
[17] J.Y. Chen, L.P. Wang, K.Y. Fu, N. Huang, Y. Leng, Y.X. Leng, P. Yang, J. Wang, G.J. Wan, H. Sun, X.B. Tian, P.K. Chu, Surf. Coat. Technol. 156 (2002) 289.
[18] J.Y. Chen, Y.X. Leng, X.B. Tian, L.P. Wang, N. Huang, P.K. Chu, P. Yang, Biomaterials 23 (2002) 2545.
[19] Y.X. Leng, J.Y. Chen, P. Yang, H. Sun, N. Huang, Surf. Coat. Technol. 166 (2003) 176.
[20] Y.X. Leng, J.Y. Chen, P. Yang, H. Sun, G.J. Wan, N. Huang, Surf. Sci. 531 (2003) 177.
[21] Diana Mardare, C. Baban, Raluca. Gavrila, M. Modreanu, G.I. Rusu, Surf. Sci. 507–510 (2002) 468.
[22] K.L. Chopra, Thin Film Phenomena, Mcgraw-Hill, New York, 1969.
[23] L. Maissel, R. Glang (Eds.), Handbook of Thin Film Technology, Mcgraw-Hill, New York, 1970.